# Experimental research on the sampling point number of LAMOST active optics wavefront test

Yong Zhang*[a]
[a]National Astronomical Observatories / Nanjing Institute of Astronomical Optics and Technology, Chinese Academy of Sciences, No.188, Bancang Street, Nanjing 210042, P. R. China

## ABSTRACT

As is known to all, the LAMOST active optics wavefront test is realized by Shack-Hartmann Wavefront Sensor. But because of the characteristics and difficulties of the LAMOST, it is the key problem in the design of LAMOST Shack-Hartmann Wavefront Sensor to select and decide the sampling point number corresponding to one segment of LAMOST. In this paper we mainly discuss the sampling point number experiment by simulating different numbers of Shack-Hartmann sampling points from one LAMOST segment based on the Large Aperture Active Optics Experiment Telescope Device, which is briefly introduced with LAMOST. After the introduction, the main contents of this article are given including the following three experimental analysis parts. The first experimental analysis is the active optics tests, active optics close loop corrections and comparisons among experiments with different sampling point numbers. The second is the fitting and correction of the low-frequency aberration items existing in the system with about twenty sampling points. The last is that the low-frequency aberrations such as astigmatism and defocus are generated and then corrected with only twenty sampling points after close loop correction with all sampling points. Finally some primary conclusions of LAMOST Shack-Hartmann Wavefront Sensor sampling point number are reached and given.

**Keywords:** Active optics, LAMOST, Shack-Hartmann wavefront sensor

## 1. INTRODUCTION

Large Sky Area Multi-Object Fiber Spectroscopic Telescope (LAMOST)[1-6] is a meridian reflecting Schmidt telescope laid down on the ground with its optical axis fixed in the meridian plane. It consists of a reflecting Schmidt corrector MA at the northern end, a spherical primary mirror MB at the southern end and a focal plane in between. Combining both the thin mirror and segmented mirror active optics, LAMOST not only controls the aspherical shape of the corrector to correct the spherical aberration of the primary mirror, but also controls the co-focus of all sub-mirrors. To approach the real application and optimize the design of LAMOST, an outdoor experiment, Large Aperture Active Optics Experimental Telescope [7-11], with full scale but unit optical components started in spring of 2001 in Nanjing. It is expected to get some results and make decision for the specification and detail design of LAMOST from this system. A Shack-Hartmann wavefront sensor (S-H WFS) is mounted on the focal platform to test the shape of the Schmidt plate Mirror A. S-H test has been widely used in optical shop testing and in telescopes, especially in active optics and adaptive optics. It mainly includes the measurement of the coordinate differences of the S-H grid and a further numerical reconstruction. Enclosure seeing here is a very serious problem because of the long light path near the ground. The thin mirror active optics correcting precision is greatly influenced by the seeing, which is also measured by the S-H WFS. Active optics in LAMOST is adopted to correct the low frequency errors lying in the system and realize the correction of the three-order spherical aberration of the primary mirror and the cofocus of both the Schmidt plate and the primary mirror. For example, there are gravitational deformations, thermal deformations and other low frequency errors caused by the mechanical adjustment.

Both the sampling point number and the measuring precision of the S-H WFS have relations with the star magnitude of the observed star. To understand the relations between the sampling points and fitting precision during the fitting of the aspheric shape of MA with Quasi-Zernike polynomials, Prof. Yanan Wang has carried out a serie of the calculations [12-15]. Fitting of the MA aspheric shape has been done with different sampling point numbers of 9, 11, 12, 13, 19, 21, 33, 85 and 217 and with simulations of different error distributions. The maximum of the error has been decided first and the

*yzh@niaot.ac.cn; phone 86 25 85482271; fax 86 25 85405562

Ground-based and Airborne Telescopes, edited by Larry M. Stepp, Proc. of SPIE
Vol. 6267, 626735, (2006) · 0277-786X/06/$15 · doi: 10.1117/12.669458

has been assigned to each point randomly. After normal slope of each point is solved and then these errors are added, the fitting by least square method is carried out. From Table.1 the fitting results of 21 are given with the maximum errors of 0.3″ and 0.2″. For each point distribution and for each error maximum, several different random error distributions have been calculated. In above table, for each point distribution, results of three kinds of error distributions are listed. The first two rows in the table is the results of given errors, where the first row is the maximum of normal angle errors and the second is the root mean square of each kind of error distribution. The following rows give the root mean square of normal angle error from each sub-mirror after fitting. From these results, we can find out that the fitting errors of 33 and 22 points are almost the same and they also have relations with the detailed error distribution. While the point number is raised to 85, the precision is improved obviously. With the maximum error of 0.3″ and with 21 points, the fitting precision is about 0.15″. Therefore the sampling point number should not be very small and it should be comparable with the number of the force actuators.

Table.1 21 points

| Errors | Maximum | 0.3″ | | | 0.2″ | | |
|---|---|---|---|---|---|---|---|
| | RMS | 0.1920 | 0.1870 | 0.1599 | 0.1108 | 0.1169 | 0.1142 |
| The root mean square of normal angle error of each sub-mirror after fitting | 1 | 0.1490 | 0.1048 | 0.0851 | 0.0940 | 0.0768 | 0.0725 |
| | 2 | 0.1485 | 0.1021 | 0.0852 | 0.0949 | 0.0767 | 0.0727 |
| | 3 | 0.1496 | 0.1106 | 0.0851 | 0.0895 | 0.0770 | 0.0726 |
| | 4 | 0.1495 | 0.1094 | 0.0851 | 0.0909 | 0.0770 | 0.0725 |
| | 5 | 0.1491 | 0.1056 | 0.0845 | 0.0945 | 0.0769 | 0.0724 |
| | 6 | 0.1487 | 0.1024 | 0.0846 | 0.0947 | 0.0768 | 0.0726 |
| | 7 | 0.1437 | 0.1750 | 0.1236 | 0.0958 | 0.0798 | 0.0829 |
| | 8 | 0.1497 | 0.1106 | 0.0847 | 0.0894 | 0.0771 | 0.0726 |
| | 9 | 0.1497 | 0.1105 | 0.0847 | 0.0910 | 0.0771 | 0.0725 |
| | 10 | 0.1393 | 0.1068 | 0.0850 | 0.0949 | 0.0859 | 0.0638 |
| | 11 | 0.1391 | 0.1057 | 0.0854 | 0.0961 | 0.0858 | 0.0638 |
| | 12 | 0.1378 | 0.1013 | 0.0938 | 0.1043 | 0.0850 | 0.0650 |
| | 13 | 0.1400 | 0.1360 | 0.0904 | 0.0851 | 0.0882 | 0.0643 |
| | 14 | 0.1399 | 0.1129 | 0.0848 | 0.0907 | 0.0863 | 0.0637 |
| | 15 | 0.1397 | 0.1110 | 0.0847 | 0.0917 | 0.0862 | 0.0637 |
| | 16 | 0.1484 | 0.1076 | 0.0875 | 0.0957 | 0.0773 | 0.0717 |
| | 17 | 0.1485 | 0.1087 | 0.0882 | 0.0977 | 0.0773 | 0.0716 |
| | 18 | 0.1459 | 0.1747 | 0.1252 | 0.0917 | 0.0813 | 0.0825 |
| | 19 | 0.1491 | 0.1170 | 0.0883 | 0.0917 | 0.0778 | 0.0716 |
| | 20 | 0.1489 | 0.1127 | 0.0875 | 0.0921 | 0.0775 | 0.0717 |
| | 21 | 0.1490 | 0.1088 | 0.0870 | 0.0958 | 0.0771 | 0.0719 |
| | 22 | 0.1490 | 0.1087 | 0.0874 | 0.0981 | 0.0771 | 0.0719 |
| | 23 | 0.1494 | 0.1174 | 0.0878 | 0.0916 | 0.0776 | 0.0718 |
| | 24 | 0.1493 | 0.1135 | 0.0871 | 0.0925 | 0.0774 | 0.0719 |

## 2. EXPERIMENTAL SYSTEM DESCRIPTION [16]

Fig.1 shows the overview of the LAMOST active optics experiment system. The point light come from S-H WFS to spherical MB Mirror, reflected to a parallel light, reflected by MA plate, and then converged to S-H wave front sensor. In this experiment system, light path is 120 meters in self-collimation close-loop correction mode, double the distance in LAMOST real observing mode. The light path is only about 6m above ground, with surrounding a lot of trees and high buildings. All these result in very serious air disturbance and very bad enclosure seeing, and they have the most key influences over the success of our active optics experiment, which is in great need of high precision.

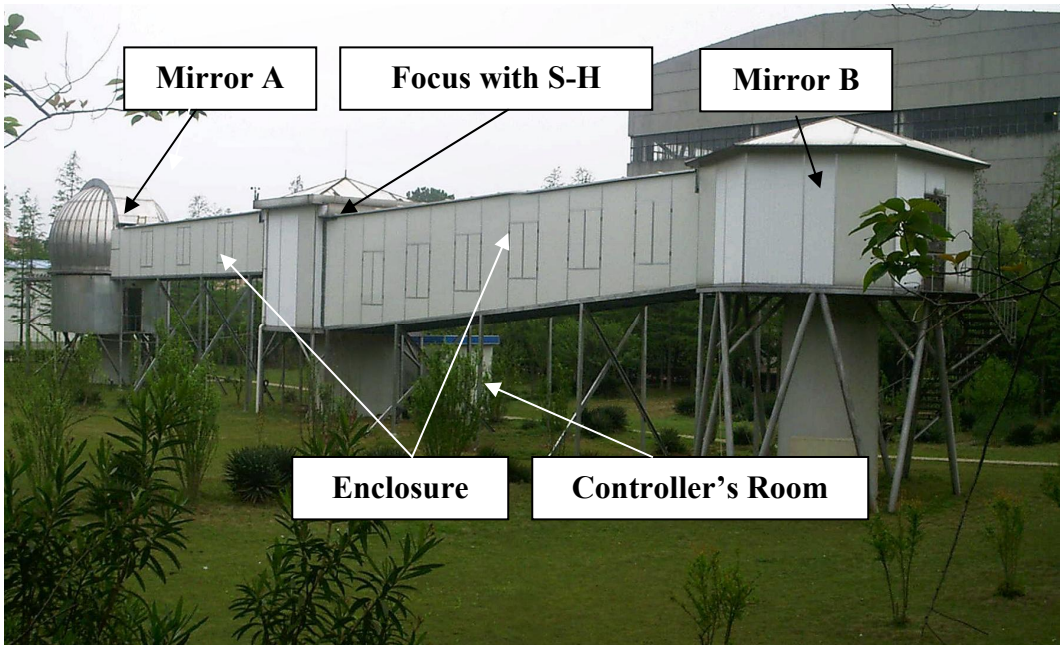


Fig.1 LAMOST outdoor experiment system overview

The sampling point pattern from the S-H WFS of the LAMOST active optics experiment system are given below Fig.2.

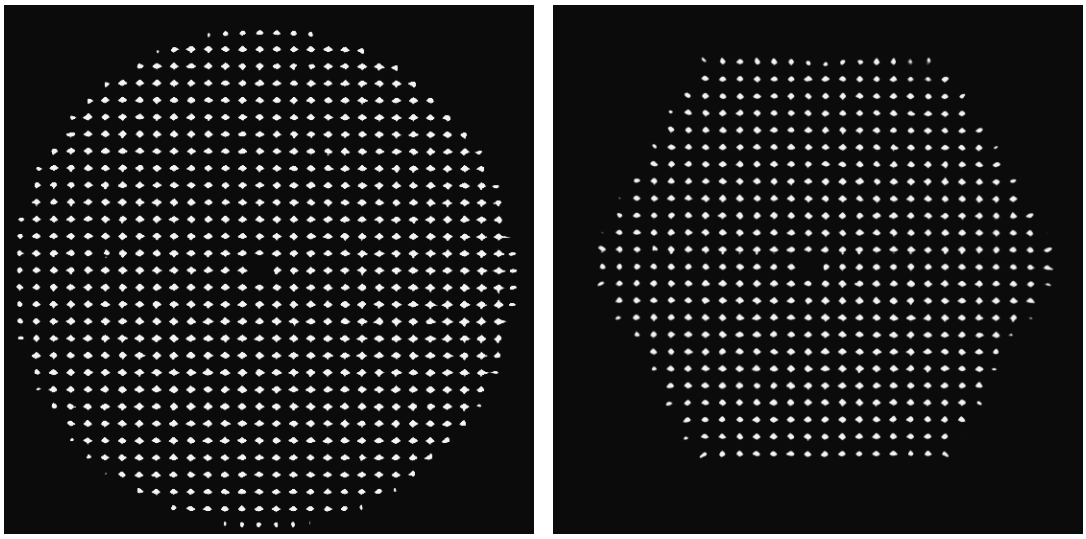

Fig.2 Sampling point pattern reference light and autocollimation light of S-H WFS

During actual experiments, methods to eliminate the sampling points and to simulate different points are described below Fig.3 and Table.2.

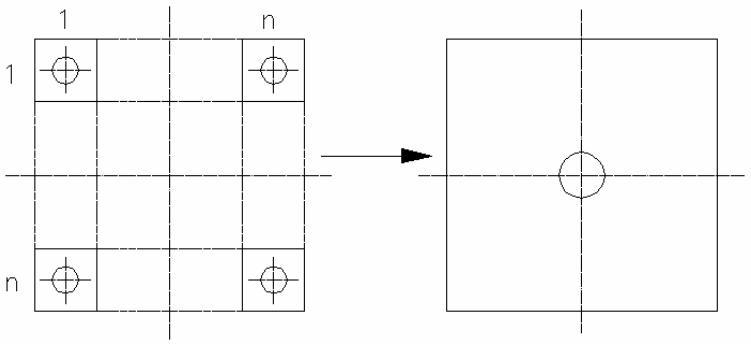


Fig.3 Sketch map of the method to eliminate sampling points by n×n square array slope averaging

Table.2 Definition of Eliminating operation Code

| Eliminating operation Code (n×n) | Content |
|---|---|
| 1×1 | No Elimination |
| 2×2 | Averaging to a sampling point every 2×2 sampling point square |
| 3×3 | Averaging to a sampling point every 3×3 sampling point square |
| 4×4 | Averaging to a sampling point every 4×4 sampling point square |
| 5×5 | Averaging to a sampling point every 5×5 sampling point square |
| 6×6 | Averaging to a sampling point every 6×6 sampling point square |

* Averaging means to describe the slopes of all sampling points in the square array by the mean slope of the central position of the square array.

Because of the discontinuity of the above the eliminating method, the sampling point number chose and used during the experiment may be discrete and the sampling point number is not adjustable continuously.

## 3. EXPERIMENTAL RESULTS

Besides the above simulation results, many further experiments have also been carried out to verify the feasibility of different numbers, especially 20, of sampling points of S-H WFS. Detailed experimental results for sampling point number selection will be given below.

### 3.1 Experimental analysis I

The first experiment is to do the active optics tests, close loop corrections and comparisons among experiments with different sampling point numbers. It was done on 18 Jan. 2005, the autocollimation seeing FWHM range is from 2.31″to 4.64″, and its mean value is 2.88″.

#### 3.1.1 Sampling point number range [50,60]

Here the Eliminating operation Code is 3×3, sampling point number range is about from 50 to 60. After only two iterative close loop corrections, three sets of data (a, b and c) are sampled and the remaining wavefront results after fitting out the wavefront tip/tilt are given below.

a: PTV=0.7485μm, RMS=0.1457μm, E80%=0.847″, Sampling point number 52.

b: PTV=0.7715μm, RMS=0.1947μm, E80%=1.075″, Sampling point number 52.

c: PTV=0.8189μm, RMS=0.1765μm, E80%=0.973″, Sampling point number 52.

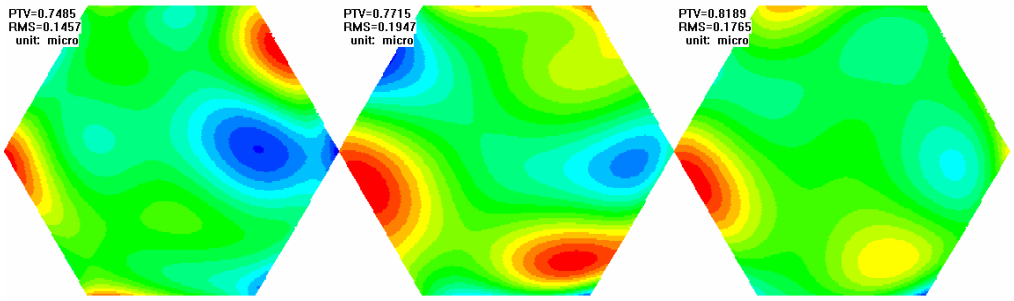


Fig.4 Wavefront maps of three wavefront results (a, b and c) (sampling point number 52)

The above wavefront shapes are inconsistent and there exists relatively large high frequency error. To verify the effect of the close loop correction, the above data are calculated to solve the wavefront with all sampling point number (n equals to 475), and remaining wavefront results after fitting out the wavefront tip/tilt are given below:

a: PTV=0.8668μm, RMS=0.1513μm, E80%=0.838″, Sampling point number 475.

b: PTV=0.9417μm, RMS=0.2079μm, E80%=1.089″, Sampling point number 475.

c: PTV=0.8334μm, RMS=0.1847μm, E80%=1.018″, Sampling point number 475.

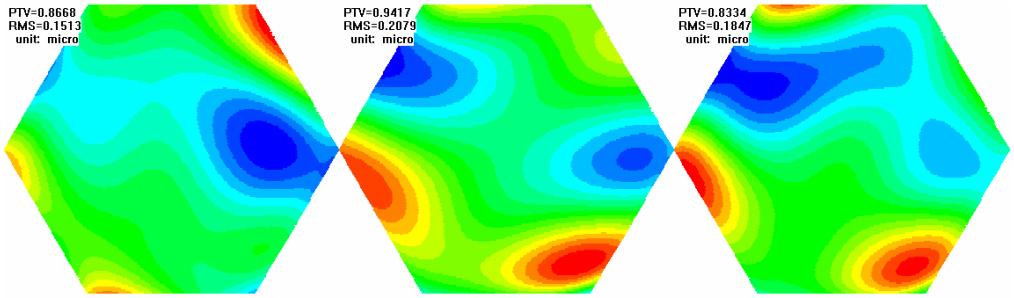


Fig.5 Wavefront maps of three wavefront results (a, b and c) (sampling point number 475)

The result differences are given to compare the different sampling point number 52 and 475.

a: PTV=0.2120μm, RMS=0.03391μm, E80%=0.2473″.

b: PTV=0.2282μm, RMS=0.02889μm, E80%=0.2233″.

c: PTV=0.4849μm, RMS=0.03566μm, E80%=0.2222″.

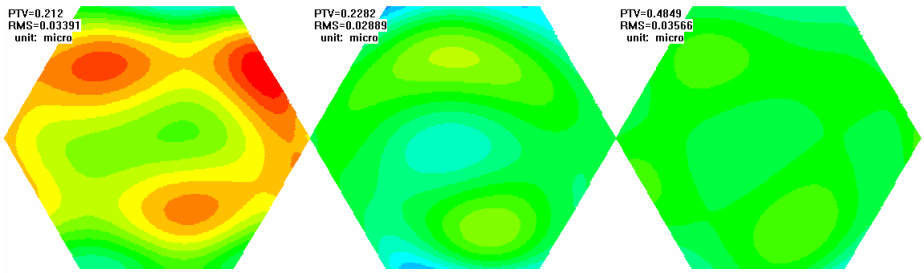


Fig.6 Wavefront differences between 52 sampling points and all sampling points (a, b and c)

From above results, the mean wavefront difference is about 0.24″of autocollimation close loop effect between 50 sampling points and almost 500 sampling points. It is comparably small.

### 3.1.2 Sampling point number range [20,30]

Here the Eliminating operation Code is 4×4, sampling number range is about from 20 to 30. After four iterative close loop corrections, three sets of data (a, b and c) are sampled and the remaining wavefront results after fitting out the wavefront tip/tilt are given below.

a: PTV=0.4408μm, RMS=0.1105μm, E80%=0.684″, Sampling point number 27.

b: PTV=0.8474μm, RMS=0.2221μm, E80%=0.946″, Sampling point number 27.

c: PTV=1.1869μm, RMS=0.3827μm, E80%=1.540″, Sampling point number 27.

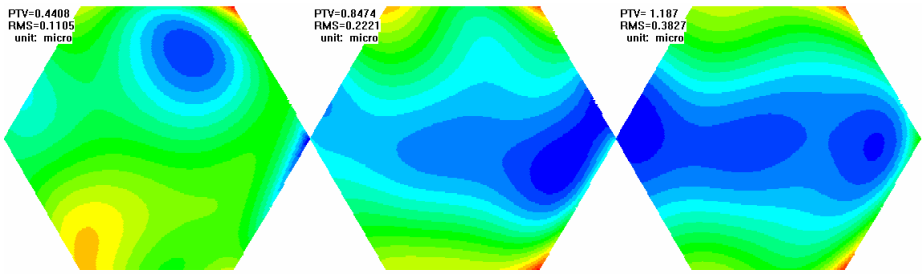


Fig.7 Wavefront maps of three wavefront results (a, band c) (sampling point number 27)

The above wavefront shapes are inconsistent and there exists relatively large high frequency error. To verify the effect of the close loop correction, the above data are calculated to solve the wavefront with all sampling point number (n equals to 478), and remaining wavefront results after fitting out the wavefront tip/tilt are given below:

a: PTV=1.0445μm, RMS=0.2058μm, E80%=1.25″, Sampling point number 478.

b: PTV=1.5903μm, RMS=0.3142μm, E80%=1.65″, Sampling point number 478.

c: PTV=1.9546μm, RMS=0.4709μm, E80%=2.05″, Sampling point number 478.

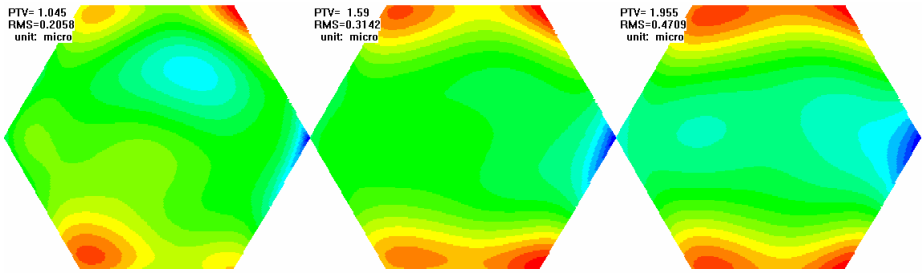


Fig.8 Wavefront maps of three wavefront results (a, band c) (sampling point number 478)

The result differences are given to compare the different sampling point number 27 and 478. From above figures, wavefronts after correction change gradually worse and fringe part of the measured wavefront with 27 sampling points has a very severe error.

a: PTV=0.5098μm, RMS=0.06718μm, E80%=0.4886″.

b: PTV=0.7975μm, RMS=0.08577μm, E80%=0.5544″.

c: PTV=0.3966μm, RMS=0.06923μm, E80%=0.3906″.

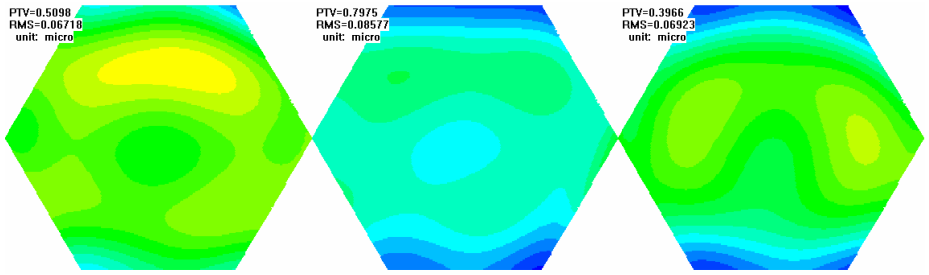


Fig.9 Wavefront differences between 27 sampling points and all sampling points (a, band c)

The mean wavefront difference is about 0.48″of autocollimation close loop effect between 27 and 478 sampling points, and it is almost twice that of the 52 sampling points.

### 3.2 **Experimental analysis II**

The second experiment is to do the fitting and correction of the low-frequency aberration items existing in the system with about twenty sampling points. Experiment was done at 28 Jan. 2005, the autocollimation seeing FWHM range is from 3.21″to 4.93″, and its mean value is 3.98″.

From Experiment I, the test and correction by S-H WFS can be realized with about 50 sampling points, and while the sampling point number decreases to about 20, the test error is ulteriorly enlarged and it cannot satisfy our demand. As we know, when sampling points decrease, the spatial frequency, which can be tested and corrected by the active optics, is reduced with them. That is to say, the ability to correct aberration shifts from spatial high frequency to spatial low frequency. The reason why the ideal precision, which is comparative with the seeing condition, cannot be obtained with comparably a few sampling points is probably that the remaining high frequency error is very large. Therefore if about 20 sampling points are used to fit and to correct the low frequency aberrations in the system, and the remaining low frequency error difference after correction between about 20 sampling points and all sampling points are compared in order to estimate the ability to correct low frequency aberrations with about 20 points.

#### 3.2.1 **Six low frequency items**

The six low frequency items used here are defocus (2,0), astigmatism (2,2), coma (3,1), three-order spherical aberrations (4,0) and (4,2). After many iterative corrections, the remaining wavefront results with different sampling point numbers by fitting with only above six low frequency items are calculated below.

I: PTV=1.044μm, RMS=0.1994μm, Sampling point number m=18.

II: PTV=3.261μm, RMS=0.5764μm, Sampling point number n=439.

I – II: PTV=1.285μm, RMS=0.2282μm, E80%=1.2895″.

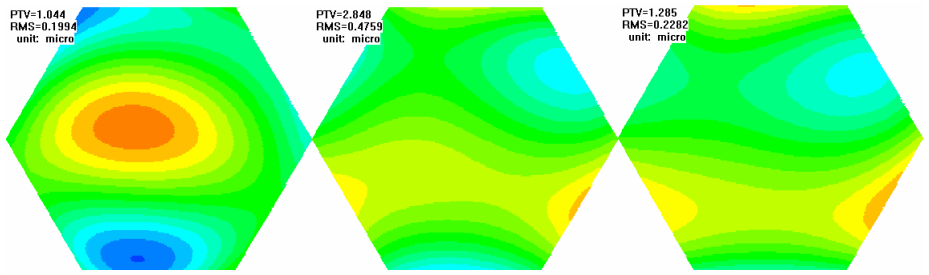


Fig.10 Wavefront of 18 and 439 points by fitting six low frequency items and their difference

From the above results, the remaining wavefront error difference with different sampling points after correction fitted with only six low frequency items is very large. That is to say, when the sampling point number is very small, the fitting error from six low frequency items is influenced greatly by the remaining high frequency error. So simulations fitting with much less low frequency items should be carried out.

3.2.2 **Simulation of three low frequency items**

There are about 20 sampling points. The three low frequency items are defocus (2, 0), astigmatism (2, 2) and three-order spherical aberrations (4, 0).

Applying the above data after correction, the remaining wavefront results with different sampling point numbers after fitting with only above three low frequency items are calculated below.

I: PTV=0.7032μm, RMS=0.1622μm, Sampling point number m=18.

II: PTV=0.5179μm, RMS=0.1305μm, Sampling point number n=439.

I - II: PTV=0.2945μm, RMS=0.0624μm, E80%=0.2567″.

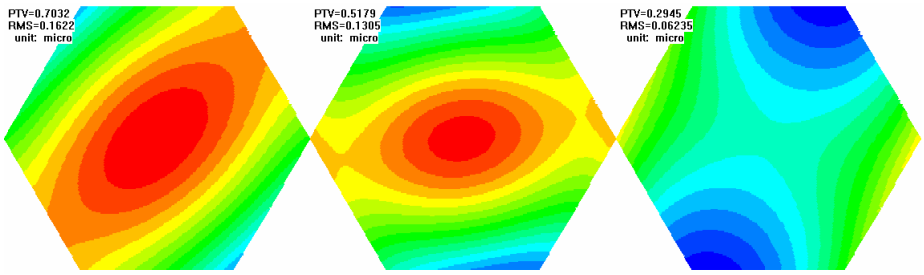


Fig.11 wavefront maps of 18 sampling points and 439 sampling points by fitting six low frequency items and their difference

From the above results, the remaining wavefront maps with different sampling points after correction with three low frequency items is very similar an their differences is also comparably small.

3.2.3 **Simulation of only one low frequency item**

During the autocollimation operations, the wavefront result is very large and it can be described with astigmatism. To find out the influence of different sampling points to above low frequency item fitting, only astigmatism item is fitted. By choosing a group of wavefront data before correction, the wavefront of different sampling point numbers fitted with astigmatism item are calculated below.

1×1: PTV=23.67μm, RMS=4.786μm, Sampling point number m=402.

2×2: PTV=20.26μm, RMS=4.098μm, Sampling point number m=87.

3×3: PTV=18.06μm, RMS=3.653μm, Sampling point number m=34.

4×4: PTV=14.58μm, RMS=2.949μm, Sampling point number m=16.

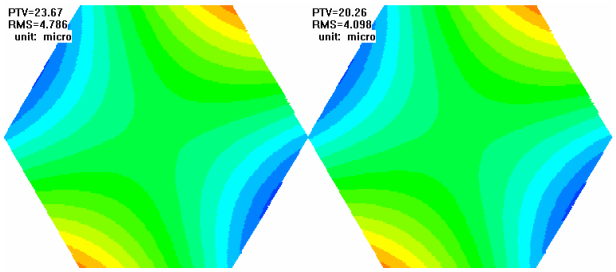


Fig.12 Astigmatism wavefront of 402 and 87 sampling points

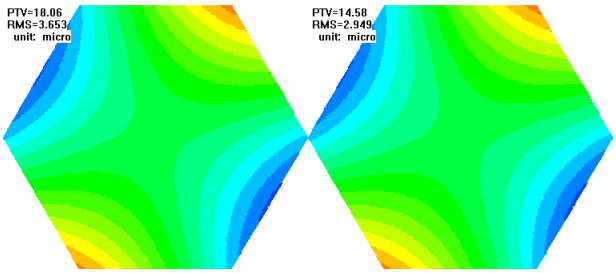


Fig.13 Astigmatism wavefront of 34 and 16 sampling points

To compare among the astigmatism wavefront results of different sampling points, differences between the latter three wavefronts and the wavefront of 402 sampling points are calculated below.

2×2 - 1×1: PTV=1.719μm, RMS=0.3479μm, E80%=1.2259″.

3×3 - 1×1: PTV=2.808μm, RMS=0.5679μm, E80%=2.0097″.

4×4 - 1×1: PTV=4.541μm, RMS=0.9185μm, E80%=3.236 ″.

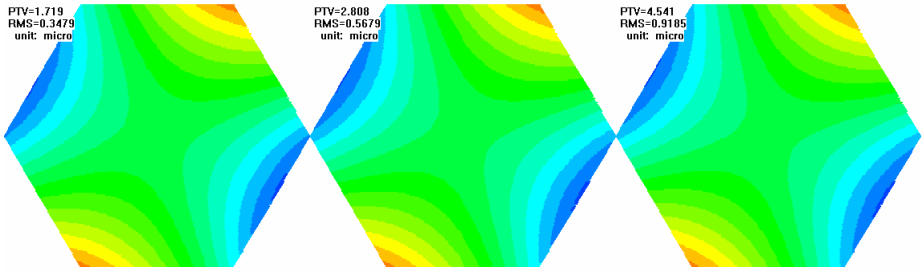


Fig.14 Astigmatism wavefront differences

### 3.3 **Experimental analysis III**

The last experiment is to generate the low-frequency aberrations such as astigmatism and defocus and then correct them with only twenty sampling points after a fine close loop correction with all sampling points. According to the discussion analysis, the results of experiment II maybe have relation with the influence of high frequency aberrations during wavefront test. For further verification of feasibility of 20 sampling points and avoiding of the influence of seeing and other high frequency aberrations in the system in order to make a correct and reasonable estimation and selection of 20 sampling points, we decide that during the days with good seeing conditions autocollimation close loop correction is carried out first with all sampling points in order to correct most high frequency aberrations as we can, then a certain quantity of low frequency aberrations such as astigmatism are generated and applied to the system. After that low frequency item fitting and close loop correction with about 20 sampling points are carried out. Finally the remaining wavefront results with just about 20 sampling points are compared with the remaining wavefront results corrected with all sampling points to verify the feasibility of low frequency aberration test and correction. Because only low frequency aberrations can be corrected with such a few sampling points, and in LAMOST active optics actual aberrations to be corrected such as Schmidt plate surface, gravitational deformation and thermal deformation are all low frequency ones, the chosen sampling point number can satisfy the demands of LAMOST if S-H WFS can correct such low frequency aberrations and obtain the precision of active optics. That is what our experiments want to be proved. The detailed results of experiments are given below.

#### 3.3.1 **Autocollimation close loop correction**

The seeing FWHM during the autocollimation mode is less than 1.83″and its mean value is 1.19″on 24 Feb. 2005. After correction with 481 sampling points, the remaining wavefront is

PTV=0.8478μm, RMS=0.1613μm, E80=0.728″, Sampling point number m=48.

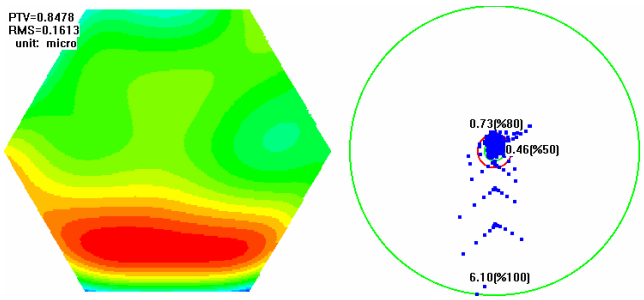


Fig.15 Wavefront and optical density after autocollimation correction (sampling point number 481)

### 3.3.2 **Generating astigmatism**

The astigmatism part to be generated, which is described to be item (2, 2) in Quasi-Zernike polynomials, is

PTV=7.836μm, RMS=1.386μm, E80=4.83″.

According to above astigmatism aberration, correcting forces can be solved by the least square method:

Maximum is 20.90N, Minimum is –30.32N.

After applying such forces, the wavefront results can be obtained.

PTV=5.3810μm, RMS=1.1366μm, E80=5.263″, Sampling point number m=443.

The generated low frequency aberration (astigmatism) mirror shape, the wavefront map and optical density map after applying the generated astigmatism are given below.

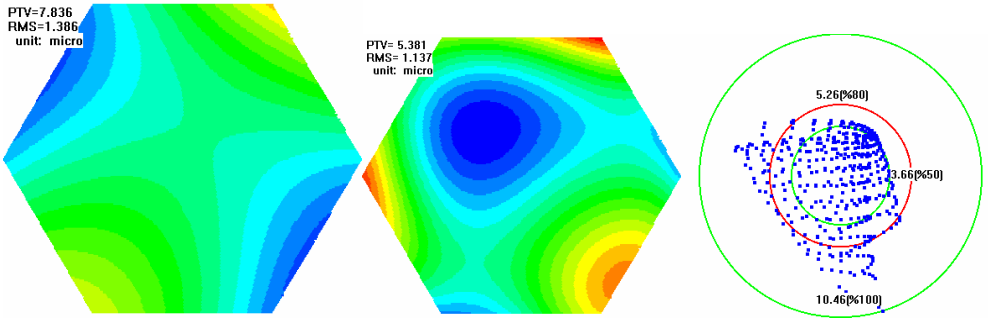


Fig.16 Generated low frequency aberration (astigmatism), wavefront and optical density after applying astigmatism (sampling point number 443)

### 3.3.3 **Low frequency close loop correction with about 20 sampling points**

After many iterative close loop corrections by fitting seven low frequency items such as (2, 0), (2, 2), (3, 1), (3, 3), (4, 0), (4, 2) and (4, 4) and by the Least Square Method, the remaining wavefront results with both 29 sampling points and all sampling points and their difference are

I： PTV=0.6654μm, RMS=0.1762μm, E80=0.917″, Sampling point number m=29.

II： PTV=1.2636μm, RMS=0.2270μm, E80=0.924″, Sampling point number m=482.

I-II： PTV=0.3758μm, RMS=0.05565μm, E80=0.2892″.

The corresponding wavefront map and optical density map are given below.

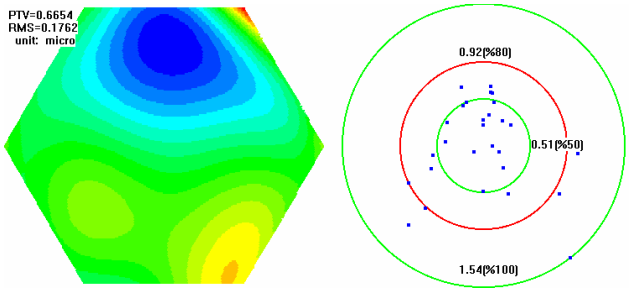


Fig.17 Remaining wavefront and optical density after correction (sampling point number 29)

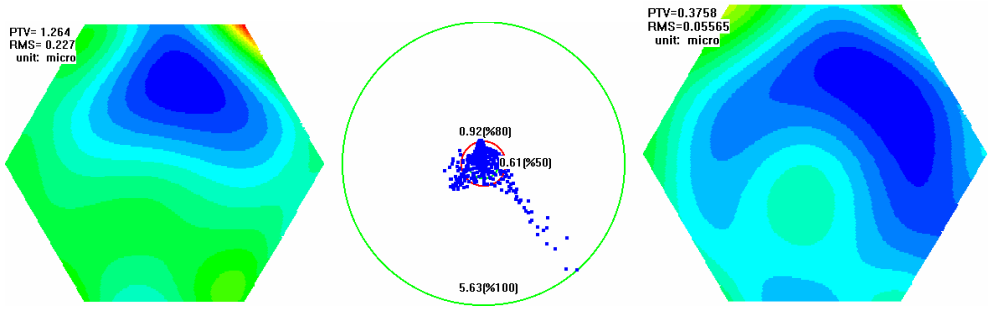


Fig.18 Remaining wavefront and optical density after correction (sampling point number 482) and the wavefront difference between sampling point number 29 and 482

## 4. CONCLUSIONS

According to above simulations and experiments, some preliminary conclusions can be obtained:

The effect difference between sampling point number 50 and 500 is only 0.24″, while the difference of sampling point number 20 is twice that of sampling point number 50. There is a comparably small segment fringe error in the remaining wavefront error of sampling point number 50. While corrected with sampling point number 28, that error turns big.

Much more iterative close loop corrections with about 20 sampling points and low frequency items, especially those specified in above Chapter 3.2.2, are needed and this kind of correction is feasible. Further more, the test error with about 20 sampling points of large astigmatism wavefront is comparably large while that of small astigmatism wavefront is small. The reason is probably because of the influence of both the fringe sampling points lose and remaining high frequency wavefront error.

Under good seeing conditions, it is proved to be adoptable that the result of many iterative low frequency close loop corrections with about 20 sampling points is close to the correction effect of adopting all sampling points, and the remaining low frequency aberration after correction is very small.

Because of not enough experiments and differences of experiments from the LAMOST actual applications, further correct conclusions can be obtained with essential further experiments.

## ACKNOWLEDGEMENT

We deeply thank our colleague, Yanan Wang, Xiangqun Cui, Yeping Li, You Wang, Xiangyan Yuan and Fang Zhou, from LAMOST project very much for their contributions and help.

## REFERENCES


1. Shou-guan Wang, Ding-qiang Su, Yao-quan Chu, Xiangqun Cui, and Ya-nan Wang, "Special configuration of a very large Schmidt telescope for extensive astronomical spectroscopic observation", Appl. Opt. Vol.35, pp 5155-5161, 1996.
2. Ding-qiang Su, Xiangqun Cui, Ya-nan Wang and Zhengqiu Yao, "Large Sky Area Multi-object Fiber Spectroscopic Telescope (LAMOST) and its key technology", SPIE Vol. 3352, Advanced Technology Optical/IRTelescopes VI, ed. by L. M. Stepp, pp. 76-90, 1998.
3. Xiangqun Cui, Ding-qiang Su, and Ya-nan Wang, "Progress in LAMOST optical system", SPIE Vol.4003, Optical Design, Materials, Fabrication, and Maintenance, ed. by P. Dierickx, pp.347-354, 2000.
4. Ding−qiang Su, Sheng−tao Jiang, Wei−yao Zou, Shi−mo Yang, Shu−ying Yang, Hai−ying Zhang, and Qi−chao Zhu, "Experiment system of thin−mirror active optics", SPIE Vol. 2199, Advanced Technology Optical Telescopes V, ed. by L. M. Stepp, pp. 609−621, 1994.
5. Ding-qiang Su, Wei-yao Zou, Zheng-chao Zhang , Yuan-gen Qu et al, "Experiment system of segmented-mirror active optics", SPIE Vol. 4003, Optical Design, Materials, Fabrication, and Maintenance, ed. by P. Dierickx, pp.417-425, 2000.
6. Yong Zhang and Xiang-Qun Cui, "Pre-Calibration Calculation in LAMOST Active Optics", Chinese Journal of Astronomy and Astrophysics, Vol.5, No.3, pp.302-314, 2005.
7. Xiangqun Cui, Ding-qiang Su, Guoping Li, Zhengqiu Yao, Zhengchao Zhang, Yeping Li, Yong Zhang, You Wang, Xiqi Xu, Hai Wang, "Experiment system of LAMOST active optics" , Proc. of SPIE, Vol.5489, Ground-based Telescopes, ed. by J. M. Oschmann, pp. 974-985, 2004.
8. Yong Zhang, Dehua Yang, Xiangqun Cui, "Measuring seeing with a Shack-Hartmann wave-front sensor during an active-optics experiment", Applied Optics, Vol. 43, No. 4, pp.729-734, 2004.
9. Zhengqiu Yao, Weina Hao, Fang Zhou, "Dome seeing improvement of LAMOST enclosure", SPIE Vol. 4837, Large Ground-based Telescopes, ed. by J. M. Oschmann, pp.198-205, 2002.
10. Yong Zhang, Yeping Li, Dehua Yang, Xiangqun Cui, "Some problems among LAMOST active optics wavefront test", Proc. Of Chinese Astronomical Telescope and Instrument Conference, ed. by Xiangqun Cui, pp. 239-246, 2002
11. Yeping Li, Xiangqun Cui, Yong Zhang, "Preliminary results and relative simulation analysis of LAMOST outdoor active optics experiment", Proc. Of Chinese Astronomical Telescope and Instrument Conference, ed. by Xiangqun Cui, pp. 139-150, 2002
12. Dingqiang Su, Yanan Wang, Chinese Journal of Astronomy and Astrophysics, Vol.17, No.3, pp.302-314, 1997.
13. Yannan Wang, Supplement of Chinese Journal of Astronomy and Astrophysics, Vol.20, 2000.
14. Lothar Noethe, Active Optics in Modern Large Optical Telescopes.
15. Yanan Wang, "Discussion of some problems of MA S-H wavefront sensor", private paper.
16. Yong Zhang, Yeping Li, "Influence of wavefront sampling points and its pattern centroid precision to wavefront test", private paper.